

Nanoscale

Accepted Manuscript



This is an *Accepted Manuscript*, which has been through the Royal Society of Chemistry peer review process and has been accepted for publication.

Accepted Manuscripts are published online shortly after acceptance, before technical editing, formatting and proof reading. Using this free service, authors can make their results available to the community, in citable form, before we publish the edited article. We will replace this *Accepted Manuscript* with the edited and formatted *Advance Article* as soon as it is available.

You can find more information about *Accepted Manuscripts* in the [Information for Authors](#).

Please note that technical editing may introduce minor changes to the text and/or graphics, which may alter content. The journal's standard [Terms & Conditions](#) and the [Ethical guidelines](#) still apply. In no event shall the Royal Society of Chemistry be held responsible for any errors or omissions in this *Accepted Manuscript* or any consequences arising from the use of any information it contains.



Nanoscale

PAPER

Two-dimensional materials saturable absorbers: Towards compact visible-wavelength all-fiber pulsed lasers

Zhengqian Luo^{a†}, Duanduan Wu^{a†}, Bin Xu^a, Huiying Xu^a, Zhiping Cai^{a*}, Jian Peng^b, Jian Weng^{b*}, Shuo Xu^c, Chunhui Zhu^c, Fengqiu Wang^{c*}, Zhipei Sun^d, and Han Zhang^e

Received 00th January 20xx,
Accepted 00th January 20xx

DOI: 10.1039/x0xx00000x

www.rsc.org/

Passive Q-switching or mode-locking by placing a saturable absorber inside the laser cavity is one of the most effective and popular techniques for pulse generation. However, most of the current saturable absorbers cannot well work in the visible spectral region, which seriously impedes the progress of passively Q-switched/mode-locked visible pulsed fibre lasers. Here, we report a kind of visible saturable absorbers—two-dimensional transition-metal dichalcogenides (TMDs, e.g. WS₂, MoS₂, MoSe₂), and successfully demonstrate the compact red-light Q-switched praseodymium(Pr³⁺)-doped all-fibre lasers. The passive Q-switching operation at 635 nm generates stable laser pulses with ~200 ns pulse duration, 28.7 nJ pulse energy and repetition rate from 232 to 512 kHz. This achievement is attributed to the ultrafast saturable absorption of these layered TMDs in the visible region, as well as the compact and all-fibre laser-cavity design by coating dielectric mirror on fibre end facet. This work may open a new way for next-generation high-performance pulsed laser sources in the visible (even ultraviolet) range.

Introduction

Compact and efficient visible-wavelength pulsed lasers are of great interest for various applications, including underwater detection, laser medicine, and biomedical imaging. Although visible-wavelength pulsed solid-state bulk laser systems (e.g. Ti: sapphire pumped optical parametric oscillators) have been relatively matured, limitations in terms of footprint, cost and efficiency have asked for alternative laser solutions. For some practical applications, it is highly desired that visible-wavelength pulsed sources are compact, user-friendly, low-cost and maintenance-free. Fortunately, visible pulsed all-fibre lasers could satisfy all these demands. At present, visible pulsed fibre sources are mainly based on frequency conversion techniques (e.g. fibre optical parametric oscillator¹ or supercontinuum generation^{2,3} in photonic crystal fibres⁴, frequency doubling of near-infrared fibre lasers⁵, and up-conversion fibre lasers⁶). Although these techniques, by exciting optical nonlinear processes in fibres, can indeed convert infrared pumping light into widely-tuneable visible light^{1,2}, they often suffer from low efficien-

cy, instability or complex structure. In contrast, if one combines rare-earth-doped fibre gain with Q-switching or mode-locking technologies, compact and efficient visible pulsed laser oscillators without additional frequency conversion methods could be expected and become more attractive. The main challenges for the past decades are from: 1) fabricating the low-loss visible gain fibres, 2) requiring high-power short-wavelength (ultraviolet or blue) pump laser diodes (LDs), and 3) obtaining suitable visible-available Q-switch or mode-locker. Thanks to the fast developments of soft-glass fibres (e.g. ZBLAN fibre) and high-power blue GaN LDs in recent years, the exciting progress of continuous-wave visible Pr³⁺-doped ZBLAN fibre lasers has been made⁷, but the pulsed operation of visible fibre laser is very rare⁸. Although active Q-switching by an acousto-optic modulator has been recently reported in the visible wavelengths⁸, it sacrifices all-fibre structure and increase the system cost. In contrast, passive Q-switching or mode-locking could be preferred, and this is therefore stimulating the research on new saturable-absorption materials for passively Q-switched/mode-locked visible fibre lasers.

In recent years, photonics based on two-dimensional (2D) materials has been extensively studied⁹, and is opening up a new playground with unprecedented opportunities for novel optoelectronic applications¹⁰⁻¹⁴. In particular, it was found that 2D materials could exhibit strong optical saturable absorption because of their unique optical and electronic properties¹⁵. Current research in 2D material-based saturable absorbers (SAs) primarily focuses on graphene¹⁶⁻¹⁸, topological insulators^{19,20}, transition-metal dichalcogenides (TMDs)^{21,22} and black phosphorus²³. They have been widely used to passively Q-switch or mode-lock lasers in wide range from 800 nm

^a Department of Electronic Engineering, Xiamen University, Xiamen 361005, China. Email: zpcal@xmu.edu.cn

^b Department of Biomaterials, College of Materials, Xiamen University, Xiamen 361005, China. Email: jweng@xmu.edu.cn

^c School of Electronic Science and Engineering, Collaborative Innovation Center of Advanced Microstructures, Nanjing University, Nanjing 210023, China. Email: fwang@nju.edu.cn

^d Department of Micro- and Nanosciences, Aalto University, FI-02150 Espoo, Finland.

^e College of Optoelectronic Engineering, Shenzhen University, 518060, China.

† These authors contributed equally to this work.

Electronic Supplementary Information (ESI) available: [Supporting information.doc]. See DOI: 10.1039/x0xx00000x

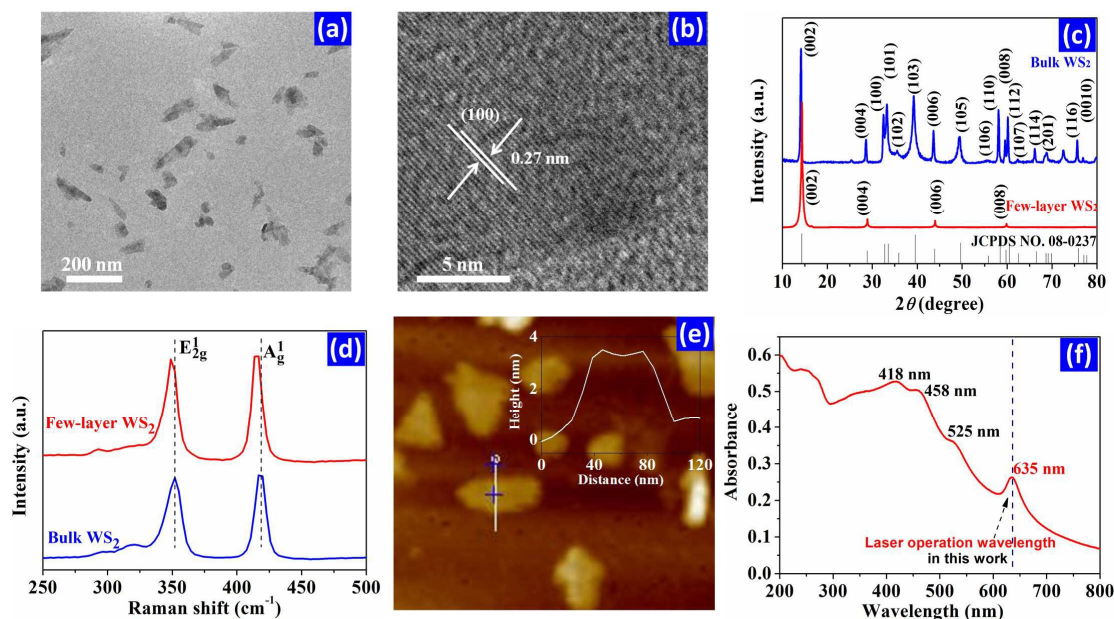


Figure 1. Characterization of few-layer WS₂. (a) TEM image. (b) HRTEM image. (c) XRD patterns of the bulk WS₂ and few-layer WS₂. (d) Raman spectra of the bulk WS₂ and few-layer WS₂. (e) AFM image. *Insert*: corresponding height profile of the few-layer WS₂ along the white line. (f) UV-vis absorption spectrum of the few-layer WS₂. The laser operation wavelength is marked as the dashed blue line.

to 3 μm ^{15, 24-28}, but all of them are still limited in the infrared wavelength operation. Up till now, 2D material-based SAs for pulsed fibre lasers have not yet become available in the visible region.

Interestingly, layered TMDs (MX₂: M=W, Mo; X=S, Se) are considered as the first type of existing 2D semiconductors with a direct bandgap at the visible frequency range²⁹, and therefore strong saturable absorption at visible wavelengths could be expected in these materials. In this article, we found that the few-layer TMDs (i.e. WS₂, MoS₂, MoSe₂) are available for visible SAs with superior performance at visible wavelength range (i.e. $\sim 7\%$ modulation depth and ~ 5 ps ultrafast relaxation time at 635 nm wavelength), well suitable for pulse generation at the visible spectral range. Furthermore, we demonstrate for the first time the visible-wavelength passively Q-switched all-fibre laser systems based on these few-layer TMDs. This approach represents a new paradigm in compact, low-cost and high-performance visible pulsed fibre laser sources for diverse applications, including underwater detection, laser medicine, biomedical imaging, and indoor optical communication.

Experimental Section

Fabrication and characterization of few-layer TMDs. The few-layer WS₂ (MoS₂ or MoSe₂) was prepared by the liquid-phase exfoliation method³⁰ (see *Methods*): The bulk WS₂ was sonicated in N-2-methyl pyrrolidone (NMP) to produce few-layer WS₂ suspension. The transmission electron microscope (TEM) image (Fig. 1a) showed that the exfoliated WS₂ was indeed thin 2D flakes. Furthermore, the distance between the adjacent hexagonal lattice fringes in the high-resolution TEM (HRTEM) image was measured to be 0.27 nm (Fig. 1b), which was consistent with the lattice space of the (100) plane.

The X-ray diffraction (XRD) pattern of the exfoliated WS₂ showed a high [002] orientation and some characteristic peaks disappeared compared to the bulk WS₂ (Fig. 1c), indicating that the bulk WS₂ had been successfully exfoliated down to few layers. The two characteristic Raman peaks at 351 and 418 cm^{-1} of the bulk WS₂ (Fig. 1d), assigned to the E_{2g}¹ and A_{1g}¹ modes respectively, were red-shifted in the exfoliated WS₂. Furthermore, the thickness of the exfoliated WS₂ nanoflakes measured by atomic force microscopy (AFM) was ~ 2 -4 nm (Fig. 1e and insert), confirming that the WS₂ nanoflakes were around 3-6 layers as the thickness of single-layer WS₂ is about 0.7 nm³¹. Moreover, the exfoliated WS₂ dispersion showed several distinct but well-defined absorption peaks³² (e.g. 635 nm, matching perfectly with our laser operation wavelength) in the visible region (Fig. 1f). All the results indicate that high-quality few-layer WS₂ has been successfully prepared. Few-layer MoS₂ and MoSe₂ were also prepared by using similar liquid-phase exfoliation method (*Supplementary Information*).

Nonlinear optical properties of few-layer WS₂ at visible 635 nm. To investigate the saturable absorption properties of the few-layer TMDs in the visible wavelength, open-aperture (OA) Z-scan technique (see *Methods*) was carried out at 635 nm, our red-light fibre laser operation wavelength. Nonlinear saturable absorption of all the as-prepared few-layer TMDs (WS₂, MoS₂, MoSe₂) could be observed in our experiment. Fig. 2a gives the representative results of the OA Z-scan traces for the few-layer WS₂ sample with the excitation powers of 1, 2.5 and 4 μW , respectively. The intensity-dependent transmittance of the few-layer WS₂ (i.e. as a function of position change) is clearly found, demonstrating the effective saturable absorption of the few-layer WS₂ at 635 nm. Noted the 635 nm

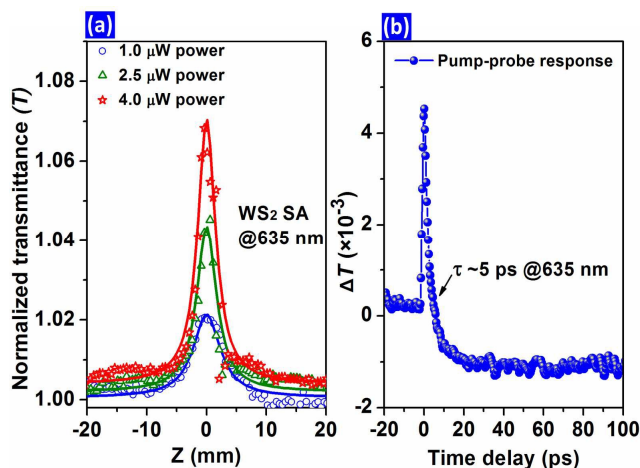


Figure 2. Nonlinear optical properties of the few-layer WS_2 at 635 nm. (a) OA Z-scan traces with the excitation powers of 1, 2.5 and 4 μW , respectively. (b) Time-resolved differential transmission (ΔT) spectra with a pump fluence of $\sim 1.5 \text{ mJ}/\text{cm}^2$ using the 635 nm degenerate pump/probe.

wavelength just locates at one of the visible absorption peaks of the few-layer WS_2 (see Fig. 1f), and the resonant absorption is likely to enhance the saturable absorption at 635 nm. The slight asymmetry in the Z-scan traces is attributable to the inhomogeneity of the WS_2 sample, which was usually observed in the Z-scan measurements of layered materials³³. Furthermore, pump-probe spectroscopy (see *Methods*) was also used to investigate the temporal dynamics of nonlinear optical properties of the few-layer TMDs. Using 635 nm degenerate pump/probe measurement, Fig. 2b shows the pump-induced change of probe transmission (ΔT) for the few-layer WS_2

sample with a pump fluence of $\sim 1.5 \text{ mJ}/\text{cm}^2$. The response exhibits an initial photobleaching (PB) signal, and quickly turns into a photoinduced absorption (PA) one. The fast PB decay is about 5 ps, showing the ultrafast response of the few-layer WS_2 at the visible 635 nm wavelength. The emerging PA could be attributed to the surface defects trapped excitons, where the increasing occupation of defective states leads to a pronounced transition to higher energy levels³⁴. In addition, we performed the same Z-scan measurement of the few-layer WS_2 at the 530 nm (green) wavelength, the strong saturable absorption was also observed (see Fig.S3 in *Supplementary Information*). The PB relaxation process combined with the OA Z-scan results, nevertheless, confirms that the few-layer WS_2 exhibits ultrafast ($\sim 5 \text{ ps}$) saturable absorption with good performance ($>7\%$ modulation depth) in the visible range, very promising for pulse generation at visible spectral range.

Results and Discussions

Experimental demonstration of TMDs-based passively Q-switched visible fibre lasers. We further present the experimental demonstration of passively Q-switched visible fibre lasers based on the few-layer WS_2 , MoS_2 and MoSe_2 , respectively. A photograph for this study is given in Fig. 3a, and the corresponding schematic of the experimental setup is shown in Fig. 3b. A piece of 98.5 cm Pr^{3+} -doped ZBLAN glass fibre (core/cladding: 6/125 μm , Pr^{3+} concentration: 1000 ppm) as visible gain medium was pumped by a 445 nm/2 W GaN LD³⁵. The end facets of the ZBLAN fibre were perpendicularly polished, and induce $\sim 4\%$ Fresnel reflection. The 445 nm pumping beam was firstly expanded by two optical lenses (L1&L2)

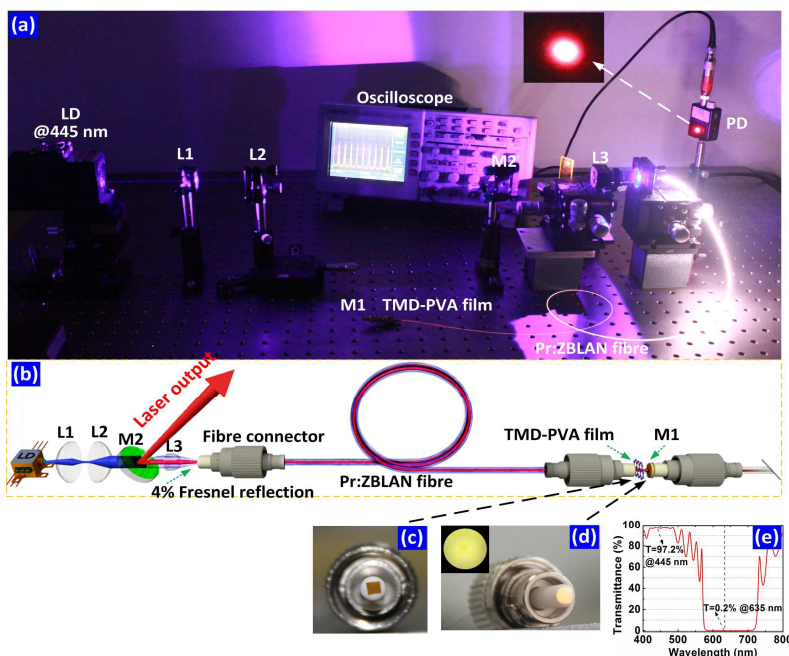


Figure 3. Experimental setup and designs of the TMDs-based passively Q-switched visible (red) fibre laser. (a) Photograph of the passively Q-switched visible fibre laser. Inset: the output beam spot. (b) Schematic of the visible fibre laser. (c) TMD-PVA film transferred on a ferrule of fibre connector. (d) High-reflective dielectric films coated on a fibre ferrule (i.e. M1), inset: the close look of the dielectric film on fibre end. (e) Optical transmission spectrum of the dielectric films. L1, L2 and L3: lens. PD: photodetector.

with different focal lengths, and then coupled into the core area of the ZBLAN fibre by a micro-objective lens (L3). The all-fibre based compact laser cavity for red-light oscillation was formed by the 4% Fresnel reflection of the ZBLAN fibre end-facet (left) and a fibre pigtail mirror M1 (right). The M1 was fabricated by directly coating multiple-layer dielectric films onto a fibre ferrule using a plasma sputter deposition system (see *Methods*). As seen in Fig. 3d, the dielectric films have been uniformly deposited on the fibre ferrule, and has a high transmittance of 97.2% at the pump wavelength of 445 nm as well as high reflectivity of 99.8% at the wavelength range of 580~710 nm (e.g. $T=0.2\%$ @635 nm, see Fig. 3e). Although the wide-waveband reflection of the M1 covers a few of emission spectral peaks (see Fig. S4 in *Supplementary Information*) of the Pr^{3+} -doped ZBLAN fiber, the laser resonator could still operate around 635 nm only, because the gain competition always leads to the oscillation at the strongest gain peak (i.e. ~635 nm). In order to realize compact and stable visible-wavelength passive Q-switching, the key step is to compatibly insert the as-prepared few-layer TMDs into the laser cavity. A WS_2 polyvinyl alcohol (PVA) film [see Fig. 3c] was firstly fabricated by evaporating the WS_2 /polymer composite solution to dryness, and was then sandwiched between the fibre pigtail mirror M1 and the Pr^{3+} -doped ZBLAN fibre end. The insertion loss of the WS_2 /polymer SA film was measured to be 2.5 dB at 635 nm, and the damage threshold is estimated to be ~1.5 GW/cm². In addition, to conveniently couple out the laser, ~96% intra-cavity oscillating light was extracted, and then reflected by an angled dichroic mirror M2 ($R>99\%$ @635 nm) as laser output. The optical spectrum of the output laser was measured by an optical spectrum analyzer, and the pulsed characteristics were detected by a photodetector (PD) together with a digital oscilloscope and a radio-frequency (RF) spectrum analyzer.

Laser pulse generation at 635 nm wavelength. To confirm the significance of the TMD-based SA to passive Q-switching, we compare the laser output characteristics with and without the TMD-based SA in the cavity. Without using TMD-based SA, it is confirmed that the 635 nm red laser always operated at continuous-wave regime and no pulse train was observed. In contrast, once a TMD-based SA (i.e. WS_2 -based SA) was placed inside the laser cavity, stable pulse trains self-started at the pump power of >143.6 mW. As shown in Fig. 4a, we measured the oscilloscope traces under different pump powers. With increasing the pump power, the pulse repetition rate became larger and larger from 245.1 to 512.8 kHz while the pulse width became narrower. These phenomena are typical features of passive Q-switching²², and therefore verifying that the WS_2 -based SA plays an important role for the visible-wavelength passive Q-switching. At a pump power of 182.2 mW, we measured the typical output optical spectrum. As given in Fig. 4b, the lasing peak wavelength located at 635.1 nm with a 3-dB linewidth of 0.08 nm. As shown in Fig. 4c, we also measured the RF output spectrum of the Q-switched pulse train. The fundamental RF peak f_0 (i.e. pulse repetition rate) is 353.0 kHz, and the RF signal-to-noise ratio (SNR) is as high as 43 dB (>10⁴ contrast), indicating the good stability of the passive Q-switching operation. Furthermore, the broad-span RF output spectrum in the inset of Fig. 4c shows an RF envelope period of ~4 MHz, which is in good agreement with the measured pulse width of 244 ns in the temporal domain (according to the Fourier transform). As shown in Fig. 4d, we further recorded the pulse repetition rate and the pulse width of the visible passive Q-switching as a function of the incident pump power. The repetition rate can be widely tuned in the range of 232.7~512.8 kHz. The pulse width sharply decreased once the pump power was above the pump threshold, but remained almost unchanged when the pump power was over 180 mW. The minimum pulse width is 207 ns. In addition, the maximum average output power for the 635 nm passively Q-switched laser is 8.7 mW, and the

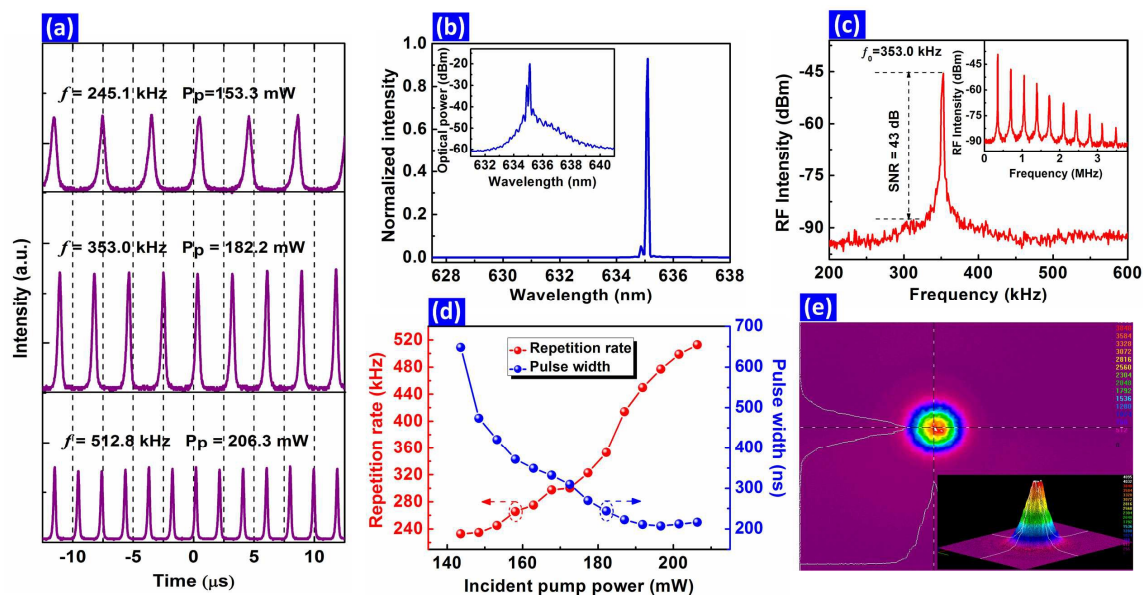


Figure 4. Experimental results of the WS_2 -based passively Q-switched visible (red) fibre laser. (a) Q-switched pulse trains under different pump powers. (b) Output optical spectrum of the Q-switching operation (inset: with dBm logarithmic scale). (c) Typical RF output spectrum of the Q-switching operation (inset: the broad-span RF output spectrum). (d) Q-switched repetition rate and pulse width vs the pump power. (e) Laser mode-field distribution.

maximum pulse energy is 28.7 nJ. In order to evaluate the output transverse-mode characteristics of the visible Q-switched fibre laser, we measured the optical intensity distribution using a laser beam analyzer (Spiricon LBA-400PC). As seen in Fig. 4e, the laser distribution from both the 2D and 3D photographs exhibit good Gaussian shape, manifesting the single-transverse-mode operation of our fibre laser.

Moreover, we also achieved the 635 nm passively Q-switched Pr³⁺-doped fibre lasers using the few-layer MoS₂ and MoSe₂ (see Fig. S5 and Fig. S6 in *Supplementary Information*), respectively. Table 1 gives a summary on the performance of passive Q-switching using different TMDs-based SAs (i.e. WS₂, MoS₂ and MoSe₂). It can be seen that their output parameters are very similar. The maximum output power (<10 mW) is relatively low, and could be further improved by optimizing the output coupling ratio and increasing the pump coupling efficiency from the blue LD into the ZBLAN fiber core.

Table 1 Performance of 635 nm passively Q-switched fiber lasers using three different TMDs-based SAs

Materials (SAs)	Lasing wavelength (nm)	Q-switched threshold (mW)	Pulse duration (ns)	Repetition rate (kHz)	Max. output power (mW)
Few-layer WS ₂	635.1	143.6	207	232.7-512.8	8.7
Few-layer MoS ₂	635.5	148.4	227	240.4-438.6	7.1
Few-layer MoSe ₂	635.4	146.8	240	357.1-555.1	6.2

One could have the concern about the fundamental mechanism of the visible-wavelength saturable absorption in the few-layer WS₂, MoS₂ and MoSe₂. Since these layered TMDs have the wide direct bandgaps²⁹ of ~2.0 eV (WS₂), ~1.9 eV (MoS₂) and ~1.5 eV (MoSe₂), respectively, their corresponding resonant wavelengths of ~620 nm (WS₂), ~690 nm (MoS₂) and ~800 nm (MoSe₂) just locate in or near the visible spectral region. Under the visible-light (e.g. 635 nm) illumination, electron-hole pairs from the layered TMDs can be in resonance (similar to carbon nanotubes¹⁵). This resonant process could make Pauli blocking very efficient, and contribute to the enhanced saturable absorption for nonlinear and ultrafast photonic applications in the visible operation wavelength.

Methods

Preparation of few-layer WS₂: The purchased bulk WS₂ (200 mg) was added into NMP (200 mL) and the solution was sonicated for 20 hours to produce the few-layer WS₂ suspension. The dispersion was then centrifuged at 2000 rpm for 30 min to remove bulk WS₂. Subsequently, the supernatant was decanted to another centrifuge tube. After centrifuging the supernatant at 13000 rpm for 30 min to remove the free NMP, the as-obtained product was collected into vials for further characterization. Finally, we collected the few-layer WS₂ suspension into vials and dispersed in polyvinyl PVA, which can be easily film-forming for further application.

Plasma sputter deposition for fibre pigtail mirror: The plasma sputter deposition system (SCT-S500) was described in the Fig. S7 in *Supplementary Information*. The plasma was initiated and amplified by a DC launch electromagnet towards the plasma source. The position of the plasma beam can be adjusted to ensure good beam impingement on the target surface. To achieve a high deposition rate in reactive process, the RF power was adjusted from 1-2.2 kW and the target negative bias voltage was set from 300-700V, respectively. During the deposition process, the system was pumped by cryo-pump with a pressure of 6×10⁻⁶ Torr. Pure argon gas was introduced to the chamber, and the oxygen was fed into the chamber. The oxygen flow was regulated from 0-30 sccm with a fixed argon flow of 85 sccm, and the background pressure is approximately 5×10⁻³ Torr. The fibre-based ferrules as the targets were used to deposit the dielectric films.

Z-scan measurement: Z-scan setup was based on a femtosecond optical parametric amplifier (OPA) which was pumped by a Ti: Sapphire amplifier system (centre wavelength: 800 nm). Specifically, we have chosen an excitation wavelength of ~635 nm to study the non-linear absorption of WS₂ samples in the visible range. The excitation pulse duration was ~100 fs (with a 1 kHz repetition rate) and a neutral density filter was employed to set the incident optical power. To avoid laser damage caused by either high peak intensity or thermal effects, we used our excitation power to <10 μW.

Pump-probe spectroscopy: For degenerate pump-probe experiment, the 635 nm femtosecond pulses were also from the OPA system used in the Z-scan. Here, the laser was split into pump and probe beam. The pump fluence is ~20 times larger than that of the probe fluence. Pump and probe beams had parallel polarization in our setup. The incident angle between pump and probe beam was smaller than 15°. To record the small change of probe beam, the fluence of probe was detected using a photo-detector and a lock-in amplifier referenced to a 500 Hz chopped pump.

Conclusions

We introduce 2D material-based SAs for all-fibre pulsed lasing in the visible regime. The red-light passive Q-switching generated the stable pulse trains with the pulse width of ~200 ns and the wide range of repetition rate from 232.7 to 512.8 kHz. The present results suggest that the layered TMDs (WS₂, MoS₂ and MoSe₂) as visible SAs are extremely effective for generating short laser pulses in the visible regime. This could mainly attribute to the wide bandgaps³⁰ (1.5~2.0 eV) of these TMDs to enhance the saturable absorption in the visible wavelength. In addition, by controlling the net dispersion of the Pr³⁺-doped ZBLAN fiber laser and optimizing the cavity designs, such layered-TMDs SAs may also enable passive mode-locking for generating ultrashort picosecond or femtosecond pulses in the visible wavelengths, and this will be our further work. In summary, this work pushed a significant step towards the new-generation, compact, low-cost and high-performance pulsed fibre laser sources in visible (even ultraviolet) wavelengths.

Acknowledgements

This work was supported by the National Nature Science Foundation of China (61275050, 61177044, 61475129, 61378025), and by the National Key Scientific Research Projects (2014CB932004, 2014CB921101) as well as the Specialized Research Fund for the Doctoral Program of Higher Education (20120121110034).

Author contributions

Z. Q. Luo and Z. P. Cai conceived of the original concept and designed the experiments. D. Wu and Z. Q. Luo performed the experiments of passively Q-switched Pr³⁺-doped fibre lasers. J. Peng and J. Weng prepared and characterized the layered TMDs. S. Xu., C. Zhu and H. Zhang contributed to the Z-scan measurements. F. Q. Wang and Z. P. Sun performed the pump-probe spectroscopy of the layered TMDs. B. Xu and H. Y. Xu contributed to the fibre pigtail mirror using the plasma sputter deposition system. All authors analyzed the experimental data. Z. Q. Luo, J. Weng, F. Q. Wang and Z. P. Sun co-wrote the paper. All authors discussed the results and revised the manuscript. Z. P. Cai and J. Weng advised on the project.

Notes and references

- J. E. Sharping, M. A. Foster, A. L. Gaeta, J. Lasri, O. Lyngnes, K. Vogel, *Opt. Express*, 2007, **15**, 1474.
- S. Coen, A. H. L. Chau, R. Leonhardt, J. D. Harvey, J. C. Knight, W. J. Wadsworth, P. S. J. Russell, *Opt. Lett.* 2001, **26**, 1356.
- J. Travers, S. Popov, J. R. Taylor, *Opt. Lett.* 2005, **30**, 3132.
- P. S. J. Russell, *Science*, 2003, **299**, 358.
- L. R. Taylor, Y. Feng, and D. B. Calia, *Opt. Express*, 2010, **18**, 8540.
- D. S. Funk, J. G. Eden, *IEEE J. Sel. Top. Quantum Electron.* 1995, **1**, 784.
- H. Okamoto, K. Kasuga, I. Hara, Y. Kubota, *Opt. Express*, 2009, **17**, 20227.
- J. Kojou, Y. Watanabe, P. Agrawal, T. Kamimura, F. Kannari, *Opt. Commun.* 2013, **290**, 136.
- A. K. Geim, K. S. Novoselov, *Nat. Mater.* 2007, **6**, 183.
- F. Bonaccorso, Z. Sun, T. Hasan, A. C. Ferrari, *Nat. Photon.* 2010, **4**, 611.
- M. Liu, X. Yin, E. Ulin-Avila, B. Geng, T. Zentgraf, L. Ju, F. Wang, X. Zhang, *Nature*, 2014, **74**, 64.
- F. Xia, T. Mueller, Y.M. Lin, A. Valdes-Garcia, P. Avouris, *Nat. Nanotechnol.* 2009, **4**, 839.
- Q. Bao, H. Zhang, B. Wang, Z. Ni, C. H. Y. X. Lim, Y. Wang, D. Y. Tang, and K. P. Loh, *Nat. Photon.* 2011, **5**, 411.
- S. Yamashita, *J. Lightwave Technol.* 2012, **30**, 427.
- A. Martinez, Z. Sun, *Nat. Photon.* 2013, **7**, 842.
- T. Hasan, Z. Sun, F. Wang, F. Bonaccorso, P. H. Tan, A. G. Rozhin, A. C. Ferrari, *Adv. Mater.* 2009, **21**, 3874.
- Q. Bao, H. Zhang, Y. Wang, Z. Ni, Y. Yan, Z. X. Shen, K. P. Loh, D. Y. Tang, *Adv. Funct. Mater.* 2009, **19**, 3077.
- C. Zaugg, Z. Sun, V. Wittwer, D. Popa, S. Milana, T. Kulmala, R. Sundaram, M. Mangold, O. Sieber, M. Golling, *Opt. Express*, 2013, **21**, 31548.
- C. Zhao, H. Zhang, X. Qi, Y. Chen, Z. Wang, S. Wen, D. Tang, *Appl. Phys. Lett.* 2012, **101**, 211106.
- J. Sotor, G. Sobon, K. M. Abramski, *Opt. Express*, 2014, **22**, 13244.
- X. Zhang, S. Zhang, C. Chang, Y. Feng, Y. Li, N. Dong, K. Wang, L. Zhong, W. J. Blau, J. Wang, *Nanoscale*, 2015, **7**, 2978.//K.
- Wang, J. Wang, J. Fan, M. Lotya, A. O'Neill, D. Fox, Y. Feng, X. Zhang, B. Jiang, Q. Zhao, *ACS Nano*, 2013, **7**, 9260.
- Z. Luo, Y. Huang, M. Zhong, Y. Li, J. Wu, B. Xu, H. Xu, Z. Cai, J. Peng, J. Weng, *J. Lightwave Technol.* 2014, **32**, 4077.
- S. Lu, L. Miao, Z. Guo, X. Qi, C. Zhao, H. Zhang, S. Wen, D. Tang, D. Fan, *Opt. Express*, 2015, **23**, 11183.
- I. H. Baek, H. W. Lee, S. Bae, B. H. Hong, Y. H. Ahn, D.-I. Yeom, F. Rotermund, *Appl. Phys. Express*, 2012, **5**, 032701.
- Z.-C. Luo, M. Liu, H. Liu, X.-W. Zheng, A.-P. Luo, C.-J. Zhao, H. Zhang, S.-C. Wen, W.-C. Xu, *Opt. Lett.* 2013, **38**, 5212.
- M. Zhang, E. Kelleher, F. Torrisi, Z. Sun, T. Hasan, D. Popa, F. Wang, A. Ferrari, S. Popov, J. Taylor, *Opt. Express*, 2012, **20**, 25077.
- N. Tolstik, E. Sorokin, and I. T. Sorokina, *Opt. Express*, 2014, **22**, 5564.
- C. Wei, X. Zhu, F. Wang, Y. Xu, K. Balakrishnan, F. Song, R. A. Norwood, N. Peyghambarian, *Opt. Lett.* 2013, **38**, 3233.
- K. F. Mak, C. Lee, J. Hone, J. Shan, T. F. Heinz, *Phys. Rev. Lett.* 2010, **105**, 136805.
- J. N. Coleman, M. Lotya, A. O'Neill, S. D. Bergin, P. J. King, U. Khan, K. Young, A. Gaucher, S. De, R. J. Smith, *Science*, 2011, **331**, 568.
- W.S. Yun, S. W. Han, S. C. Hong, I. G. Kim, J. D. Lee, *Phys. Rev. B*, 2012, **85**, 033305.
- J. Wilson, A. Yoffe, *Adv. Phys.* 1969, **18**, 193.
- H. Zhang, S. Virally, Q. Bao, K. P. Loh, S. Massar, N. Godbout, P. Kockaert, *Opt. Lett.* 2012, **37**, 1856.
- H. Shi, R. Yan, S. Bertolazzi, J. Brivio, B. Gao, A. Kis, D. Jena, H. G. Xing, L. Huang, *ACS Nano*, 2013, **7**, 1072.
- B. Xu, P. Camy, J.-L. Doualan, Z. Cai, R. Moncorgé, R. *Opt. Express*, 2011, **19**, 1191.